

Université de Mons

Faculté Polytechnique – Service de Mécanique Rationnelle, Dynamique et Vibrations

31, Bld Dolez - B-7000 MONS (Belgique)

065/37 42 15 – georges.kouroussis@umons.ac.be



L. Ben Fekih, O. Verlinden, Ch. De Fruytier, G. Kouroussis, New high cycle fatigue test facility of adhesively bonded ceramic electronic components, *Proceedings of the 15th European Conference on Spacecraft Structures, Materials and Environmental Testing*, Noordwijk (The Netherlands), 28 May – 1 June, 2018.

NEW HIGH CYCLE FATIGUE TEST FACILITY OF ADHESIVELY BONDED CERAMIC ELECTRONIC COMPONENTS

Lassaad Ben Fekih⁽¹⁾, Olivier Verlinden⁽¹⁾, Christophe De Fruytier⁽²⁾, Georges Kouroussis⁽¹⁾

⁽¹⁾ University of Mons, Place du Parc 20, 7000 Mons, Belgique, lassaad.benfekih@umons.ac.be

⁽²⁾ Thales Alenia Space Belgium, Rue Chapelle Beaussart 101, 6030 Charleroi, Belgium, christophe.defruytier@thalesalieniaspace.com

ABSTRACT

Adhesive reinforcement of pad-soldered electronic components may preclude their failure under random vibration of space vehicle launch. Before usage, adhesives need in-situ fatigue characterization. This work focuses on high cycle fatigue testing on shaker using resonant specimens. Test assemblies consist of a ceramic component adhesively bonded to a printed circuit board (PCB). Their design is intended to reproduce real service conditions of PCB uniaxial and biaxial bending. An in-house control routine permits to excite the test specimen at its resonance frequency at a user-specified PCB deflection amplitude. The control is based on the user PCB deflection input and accelerations measured at the head of the shaker and at one PCB location. Results of high cycle fatigue testing of Ablestik82 adhesive illustrate the effectiveness of the newly developed test facility.

1. INTRODUCTION

The interest in new high cycle fatigue testing techniques is on the rise [1]. This is motivated by shortened delays regarding the quantification of new equipment given the expansion of space activities. Excitation frequencies reach 100 Hz by general purpose servo-hydraulic machine, e.g., Instron 8801, 8802 [3] or by some electromechanical machines, e.g., Instron Dynapulse series [3]. In [4] a classical servo-hydraulic machine has been upgraded by use of voice coil servo-valve to reach 1000 Hz. Such achievement contributes, however, to a very limited displacement of +/- 0.1 mm. Drawbacks of traditional facilities include high power consumption, cost of the machine, as well as numerous technical difficulties related to stiffness tuning and alignment adjustment of the specimen. Besides, at high frequencies acceleration effects appear due to inertia of the load train, compensation becomes required in the control loop, also fatigue of the servo-valve itself could be expected. The current work is motivated by the availability of shakers in most space companies to produce a fatigue test facility including control and damage monitoring features at no extra cost. In so-doing it is necessary to design efficient resonant test specimens. In fact, there is a shortage in standardized ones involved in fatigue testing of electronics. Ref. [5] reported the development of a shaker test method including monitoring of the resonance frequency and damping ratio at a given vibration mode. Their experimental procedure lies in the use of a compact RIO controller cRIO-9074 (~4 k€) to generate the sine

command, and of LabView to perform control actions. A 24 bits A/D converter performs the acquisition of relative displacement between one point of the resonant structure and the vibrating head of the shaker. Control of frequency and amplitude of the command signal is performed in closed loop based on: phase shift between the two displacements and amplitude of the relative displacement between the PCB and vibrating head, respectively. Authors failed to excite the structure at its resonance frequency. Consequently, they resorted to a different excitation frequency from the resonance zone, more particularly, at a phase shift of 175°. This has led to lose quarter of the resonance amplification. Indeed, authors argued their choice by the difficulty to obtain a stable response at the resonance. Their monitoring of the resonance frequency relies on circle fit frequency modal identification method requiring, in turn, computation of the frequency response function. In [6] a commercial acquisition control peripheral software has been used to generate sine waveforms at a closed-loop-controlled acceleration amplitude and constant excitation frequency. Authors do not provide more insight about the algorithm behind. Although monitoring is not included in such system, authors managed to compute the transmissibility each 10⁴ cycles to emphasize the decrease of the resonance frequency during specimen testing. This solution may prevent the detection of rapid damage propagation as well as abrupt changes. In Ref. [7] a predefined constant acceleration amplitude swept sine profile has been produced on shaker. Control of amplitude and generation of signal have been achieved through fuzzy logic control implemented in LabVIEW environment using NI PXI-8186.

This work describes an in-house test consisting in subjecting the device under test (DUT) to a user-specified displacement amplitude and cadence adjusted at the fundamental frequency of the test specimen and in monitoring the resonance frequency of the DUT. The proof of concept of the test facility will be demonstrated through high cycle fatigue testing of printed circuit board-ceramic adhesively bonded assemblies. The latter consist of novel resonant structures loaded in bending about one axis and about two axes simultaneously referred to as uniaxial and biaxial bending, respectively.

2. EXPERIMENTAL METHOD

The experimental set-up is schematized in Fig. 1. The shaker is controlled via an in-house C++ routine. Sine waveforms are generated by a procedure under patenting process. National Instrument 16 bits, 2MS/s acquisition

card 6361 permits to measure accelerations of the head of the shaker and point of the specimen, denoted by $a_b(t)$ and $a_c(t)$, respectively. The command signal of the shaker is expressed by

$$v(t) = V(t) \sin[2\pi f(t)t] \quad (1)$$

where $V(t)$ and $f(t)$ are the amplitude and frequency of the command signal of the shaker, respectively.

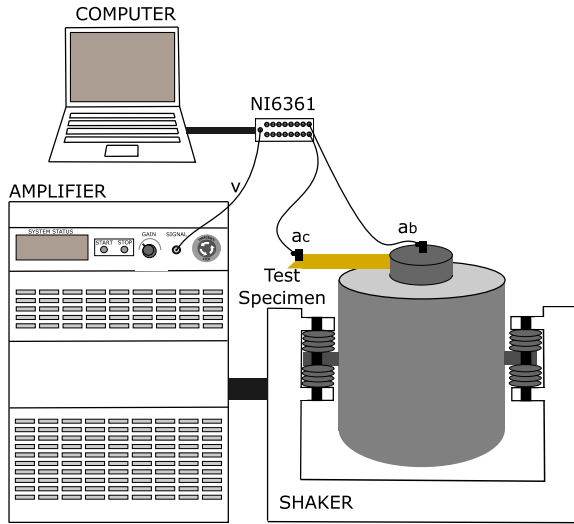


Figure 1. Illustration of the fatigue test set-up.

$f(t)$ holds continuously equal to the varying resonance frequency of the test specimen. $V(t)$ is adjusted to meet the specimen deflection specified by the user.

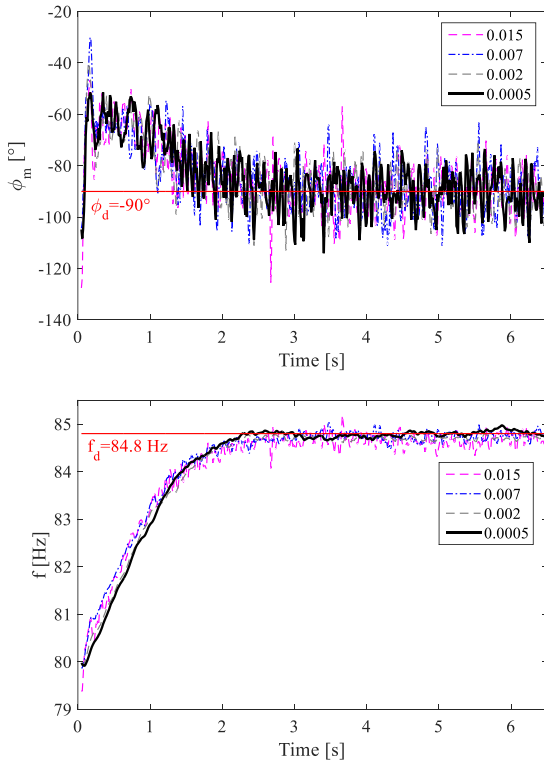


Figure 2. Optimal tuning of the frequency control without phase stabilization.

The control is exclusively based on two feedback accelerations $a_b(t)$ and $a_c(t)$. The result of the frequency control is depicted in Fig. 2 which plots the time history of (1) the phase shift between $a_b(t)$ and $a_c(t)$ and (2) the excitation frequency. After about 2s, the phase shift is equal to 90° , indicating that the resonance is reached.

3. HIGH CYCLE FATIGUE OF ABLESTIK82 STRUCTURAL ADHESIVE

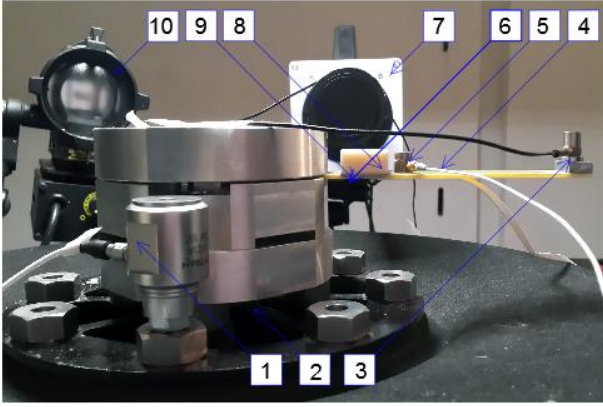
3.1. Design of Resonant Adhesively Bonded Specimens

Adhesive bonded test assemblies are composed of a PCB of most common dimension, an adhesive layer and a ceramic component made of pure alumina. Two configurations are prepared. The first set-up, illustrated in Fig. 3, is devoted to test uniaxial bending. Location of the overlap region is optimized to worst case of maximum bending moment. The same consideration applies for biaxial bending set-up where the ceramic component is bonded to center of the PCB. The second specimen was intentionally hidden for patenting reason. Acceleration responses are measured at the PCB maximum deflection location. Additional masses permit to increase the load and restrain the first resonance frequency of the assembly to 100 Hz. In practice, resonance frequencies of uniaxial and biaxial test specimens were about 50 and 60 Hz, respectively. Furthermore, special strain gages are placed at locations most appropriate to monitor the adhesive damage. It is noteworthy to mention that instrumentation and design of the present prototypes are a novelty of this work and are not standardized yet.

3.2. Experimental Fatigue Testing

A preceding quasi-static analysis figured out the elastic domain of Ablestik82 epoxy adhesive within the same prototypes. The latter span [0-15 mm] and [0-4.25 mm] of maximum PCB deflection under uniaxial and biaxial bending, respectively. Accordingly, PCB deflection levels needed for high cycle fatigue testing are known to be lower than these levels to keep linear behaviour. Under quasi-static and fatigue testing, the uniaxial set-up does not lead to a complete decohesion of the ceramic component. This drives the need to assess appropriate indicators to detect the onset of damage. Available vibratory metrics consist of the PCB backplane lengthwise strain denoted by ϵ_L , the PCB maximum warp denoted by W_m , the measured resonance frequency, f_m , and lastly the phase lag between $a_b(t)$ and $a_c(t)$ referred to as ϕ_m .

The decohesion event could be detected by a specific signature under patenting. Note that the add of an accelerometer in the vicinity of the component permits to enhance the f_m indicator. In parallel, a high speed camera has been deployed towards one extremity of the adhesive layer. The initial state of the meniscus is checked safe at glance.



1. Base accelerometer Dytran 100 mV/g
2. Head of the shaker
3. PCB accelerometer (for control) B&K 10 mV/g
4. PCB
5. PCB accelerometer (for damage monitoring) DJB 100 mV/g
6. Strain gauge Kyowa KFRP-2-120-C1-9
7. High speed camera Photron FASTCAM SA3 model 60K-M1
8. Ceramic component
9. Adhesive joint
10. Tungsten light head DLHM4-300

Figure 3. Adhesively bonded test assembly for uniaxial fatigue bending

The onset of crack appears at 61.15s or equivalently after 2966 cycles at W_d (desired PCB deflection) equal to 8 mm, as viewed from Fig. 4. This result agrees with vibratory metrics detection at 57.18 s. This matching has been obtained similarly from three specimens undergoing $W_d = 8$ mm. Thereby, the relevance of the proposed vibratory metrics could be validated. To conclude, such indicators have the advantage to be more precise, more practical and less onerous than high speed camera. It is worth noting that the detection of crack damage is still a challenging subject for the scientific community. Under biaxial testing previous indicators slightly fluctuate. Therefore, crack onset and propagation are badly separable as total decohesion occurs suddenly. The reason is in part the fragile nature of the adhesive under test.

3.3. Discussion of Results

The number of cycles to failure N_f is obtained by techniques mentioned above. The reproducibility is checked for three specimens tested at 8 mm and three others at 2 mm for uniaxial and biaxial bending, respectively. Plotted results in log-log scale are illustrated in Fig. 5. In final 8 and 11 tests have been retained amongst 10 and 15 available. Although below referred recommendation of 20 specimens, test results are not highly scattered. Data perfectly fit under either uniaxial or biaxial bending to Basquin's equation of mathematical form

$$N_f^\beta W = C \quad (2)$$

where β and C are Basquin's parameters [9].

It can be remarked that the slope of W_m vs. N_f under uniaxial bending is higher compared to biaxial bending. Thales Alenia Space Belgium requires that assembly elements, adhesive joints included, survive 10 min of under random vibration qualification. At the same time, the first resonant mode of actual PCBs occurs approximatively at 300 Hz. So, the bonded specimen should survive $N_{f,Thales} = 18E^4$ cycles. Integration of $N_{f,Thales}$ in Basquin laws permits to derive PCB deflection thresholds restricted to tested geometries of 2.49 and 1.84 mm under uniaxial and biaxial specimens, respectively.

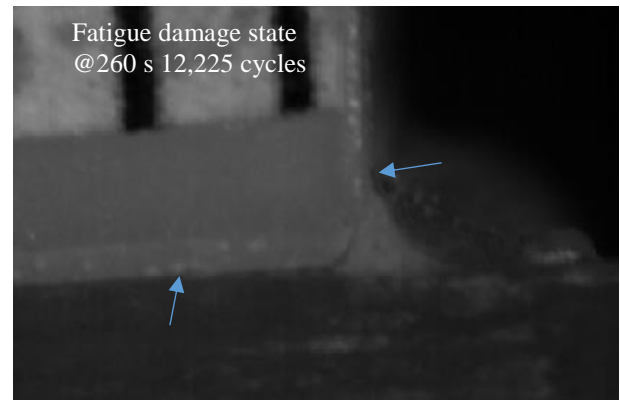
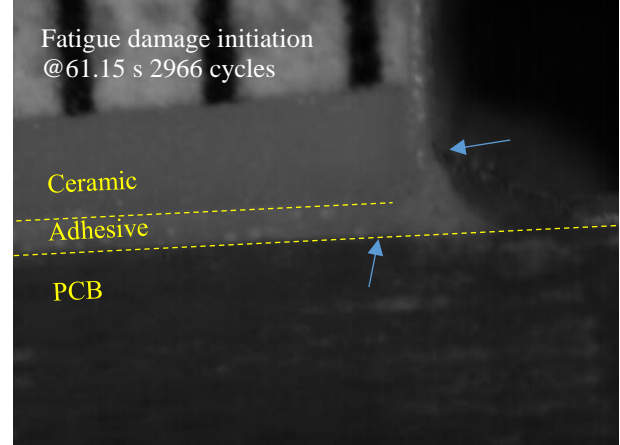


Figure 4. High speed camera inspection of adhesive joint structural integrity under fatigue cycling using uniaxial bending test specimen

Afterwards, it is possible to generalize such findings for any geometry of bonded adhesive assemblies. The idea consists in invoking Steinberg criterion of fatigue stipulating that by $W/B < 0.3\%$, the fatigue life is expected to reach empirically $N_{f,Steinberg} = 5E^8$ cycles, B being the length of the PCB [10]. Combined with the first requirement of Thales, the following relation is obtained:

$$\frac{W_{Thales}}{W_{Steinberg}} = \left(\frac{N_{f,Steinberg}}{N_{f,Thales}} \right)^{\frac{1}{\beta}} \quad (3)$$

$\frac{W_{Thales}}{W_{Steinberg}}$ can be evaluated at 0.09 and 0.39 under uniaxial and biaxial bending, respectively. Within current B dimensions this corresponds to respective threshold PCB deflections of 3.79 and 1.16 mm for $18E^4$ cycles. It can be remarked that Steinberg criterion is conservative under biaxial bending but risky under uniaxial bending. Knowing that biaxial bending is more frequently met in practice than uniaxial bending one could retain with caution the adequacy of Steinberg criterion mentioned above.

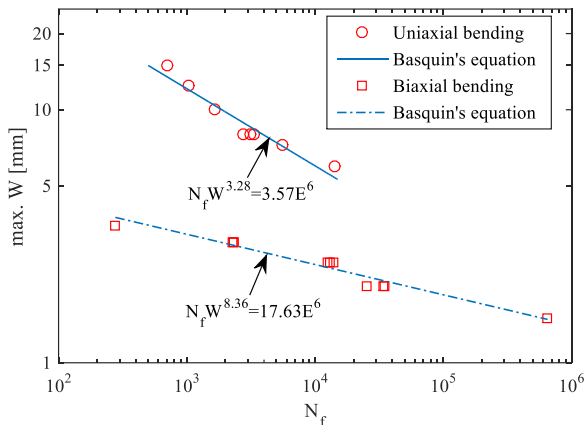


Figure 5. Fitting of Basquin's high cycle fatigue curves from experimental uniaxial and biaxial fatigue campaigns.

4. CONCLUSION

The in-house frequency and magnitude control and monitoring routine have permitted to carry out successfully fatigue testing under biaxial and uniaxial bending. Resonant test specimens have been newly designed for this purpose. The feasibility of fatigue damage onset detection has been approached by some vibratory metrics. Qualitatively, Ablestik82 adhesive has exhibited a fragile damage behaviour, overall. In uniaxial bending, the progression of damage is more obvious than in biaxial bending where total failure occurs suddenly. Quantitatively, under both loadings, PCB deflection versus the number of cycles to failure curves follow Basquin's equation. Curve's slope in uniaxial bending is higher compared to biaxial bending. Obtained curves served for deriving PCB deflection thresholds: first for the geometry of test specimens and second for any other bonded specimen geometry. The last finding stems from the application of Steinberg fatigue criterion devoted to printed circuit board. Its classical form is conservative under biaxial bending but risky for uniaxial bending. Thus, a review of the criterion threshold percentage or formulation becomes required. This is in accordance with a prior modification of the same criterion operated in quasi-static testing [11].

5. REFERENCES

1. Stanzl-Tschegg, S. (2014). Very high cycle fatigue measuring techniques. *International Journal of Fatigue*. **60**, 2–17.
2. General purpose hydraulic fatigue (2018). <http://www.instron.us/en-us/products/testing-systems/dynamic-and-fatigue-systems/servo-hydraulic-fatigue>.
3. Electropuls (2018). <http://www.instron.us/en-us/products/testing-systems/dynamic-and-fatigue-systems/electropuls-systems>.
4. Morgan, J.M. & Milligan, W.W. (1997). A 1 kKz Servohydraulic Fatigue Testing System. In Proc. 'High Cycle Fatigue of Structural Materials' (Eds. W.O. Soboyejo & T.S. Srivatsan), TMS, Warrendale PA, USA, pp305-312.
5. Česnik, M. & Slavič, J. & Boltežar, M. (2012). Uninterrupted and accelerated vibrational fatigue testing with simultaneous monitoring of the natural frequency and damping. *Journal of Sound and Vibration*. **331**(24), 5370–5382.
6. Khalij, L. & Gautrelet, Ch. & Guillet, A. (2015). Fatigue curves of a low carbon steel obtained from vibration experiments with an electrodynamic shaker. *Materials & Design*. **86**, 640–648.
7. Rana, K.P.S. (2011). Fuzzy control of an electrodynamic shaker for automotive and aerospace vibration testing. *Expert Systems with Applications*. **38**, 11335–11346.
8. Righetti, L. & Buchli, J. & Ijspeert, A. J. (2006). Dynamic Hebbian Learning in Adaptive Frequency Oscillators. *Physica D*. **216**, 269-281.
9. Ben Fekih, L. & Kouroussis, G. & Verlinden, O. (2013). Spectral-based fatigue assessment of ball grid arrays under aerospace vibratory environment. *Key Engineering Materials*. **569-570**, 425-432.
10. Steinberg, D.S. (2000). *Vibration Analysis for Electronic Equipment*. John Wiley and Sons. California, USA, 2000.
11. Ben Fekih, L. & Kouroussis, G. & Verlinden, O. (2015). Verification of empirical warp-based design criteria of space electronic boards. *Microelectronics Reliability*. **55**(12), 2786-2792.